Dentomaxillofacial Radiology, 2024, **53**, 256–266
https://doi.org/10.1093/dmfr/twae012
Advance access publication: 19 March 2024
Research Article

Artificial intelligence system for automatic maxillary sinus segmentation on cone beam computed tomography images

Ibrahim Sevki Bayrakdar, PhD[1], Nermin Sameh Elfayome, PhD[2], Reham Ashraf Hussien, PhD[2], Ibrahim Tevfik Gulsen, DDS[3], Alican Kuran, DDS[4,*], Ihsan Gunes, PhD[5], Alwaleed Al-Badr, DDS[6], Ozer Celik, PhD[7], Kaan Orhan, PhD[8]

[1]Department of Oral and Maxillofacial Radiology, Faculty of Dentistry, Eskisehir Osmangazi University, Eskisehir, 26040, Turkey
[2]Department of Oral and Maxillofacial Radiology, Faculty of Dentistry, Cairo University, Cairo, 12613, Egypt
[3]Department of Oral and Maxillofacial Radiology, Faculty of Dentistry, Alanya Alaaddin Keykubat University, Antalya, 07425, Turkey
[4]Department of Oral and Maxillofacial Radiology, Faculty of Dentistry, Kocaeli University, Kocaeli 41190, Turkey
[5]Open and Distance Education Application and Research Center, Eskisehir Technical University, Eskisehir, 26555, Turkey
[6]Restorative Dentistry, Riyadh Elm University, Riyadh, 13244, Saudi Arabia
[7]Department of Mathematics-Computer, Eskisehir Osmangazi University Faculty of Science, Eskisehir, 26040, Turkey
[8]Department of Oral and Maxillofacial Radiology, Faculty of Dentistry, Ankara University, Ankara, 06560, Turkey

*Corresponding author: Alican Kuran, DDS, Department of Oral and Maxillofacial Radiology, Faculty of Dentistry, Kocaeli University Yuvacık Campus No:7, 41190 Başiskele/Kocaeli, Turkey (alican.kuran@outlook.com)

Abstract

Objectives: The study aims to develop an artificial intelligence (AI) model based on nnU-Net v2 for automatic maxillary sinus (MS) segmentation in cone beam computed tomography (CBCT) volumes and to evaluate the performance of this model.

Methods: In 101 CBCT scans, MS were annotated using the CranioCatch labelling software (Eskisehir, Turkey) The dataset was divided into 3 parts: 80 CBCT scans for training the model, 11 CBCT scans for model validation, and 10 CBCT scans for testing the model. The model training was conducted using the nnU-Net v2 deep learning model with a learning rate of 0.00001 for 1000 epochs. The performance of the model to automatically segment the MS on CBCT scans was assessed by several parameters, including F1-score, accuracy, sensitivity, precision, area under curve (AUC), Dice coefficient (DC), 95% Hausdorff distance (95% HD), and Intersection over Union (IoU) values.

Results: F1-score, accuracy, sensitivity, precision values were found to be 0.96, 0.99, 0.96, 0.96, respectively for the successful segmentation of maxillary sinus in CBCT images. AUC, DC, 95% HD, IoU values were 0.97, 0.96, 1.19, 0.93, respectively.

Conclusions: Models based on nnU-Net v2 demonstrate the ability to segment the MS autonomously and accurately in CBCT images.

Keywords: artificial intelligence; computer modelling; deep learning; CBCT; maxillary sinus.

Introduction

The maxillary sinus (MS) is the largest of the 4 paranasal sinuses and the first to develop. The MS, a pyramid-shaped cavity, is bounded by 6 walls and shares borders with critical anatomical structures due to its location. The upper wall is bordered by the orbital cavity and infraorbital complex, the anterior wall by the infraorbital foramen and anterior superior alveolar canal, the posterior wall by the pterygopalatine fossa containing important vascular and neural structures, the lateral wall by the infratemporal fossa and posterior superior alveolar canal, and the inferior wall by the alveolar process and the roots of the maxillary teeth.[1]

Accurate visualization of the MS is crucial for precise diagnosis of symptomatic and nonsymptomatic MS pathologies, as well as for successful sinus surgical procedures in maxillofacial surgery.[2] The MS is of concern for various dental procedures, ranging from tooth extraction to implant placement, due to its proximity to the alveolar ridge and teeth. When assessing sinus status and margins during diagnosis and treatment planning, cone beam computed tomography (CBCT) is the most suitable imaging modality due to its 3D imaging capability.[3] Panoramic radiography (PR) and computed tomography (CT) are other imaging techniques commonly used in the evaluation of the maxillary sinus. PRs are commonly used due to their convenience and low radiation dose but can be difficult to interpret due to superimposition in the MS region.[4] When the sinus floor is in close proximity to the roots of the teeth on the buccal or palatal side, the roots may appear to be inside the sinus on panoramic radiographs.[5] Additionally, panoramic radiography has demonstrated poor performance in detecting sinus membrane thickening,[6] sinus septum,[7] or oroantral communication after tooth extraction.[8] Moreover, anatomical variations of the maxillary sinus may be misidentified as radicular cysts on panoramic radiographs, leading to undesired "false positive" evaluations.[9] While CT has traditionally been the preferred method for preoperative examination of the MS before implant placement, CBCT is becoming increasingly popular due to its low-dose,

Received: 17 January 2024; **Revised:** 29 February 2024; **Accepted:** 14 March 2024

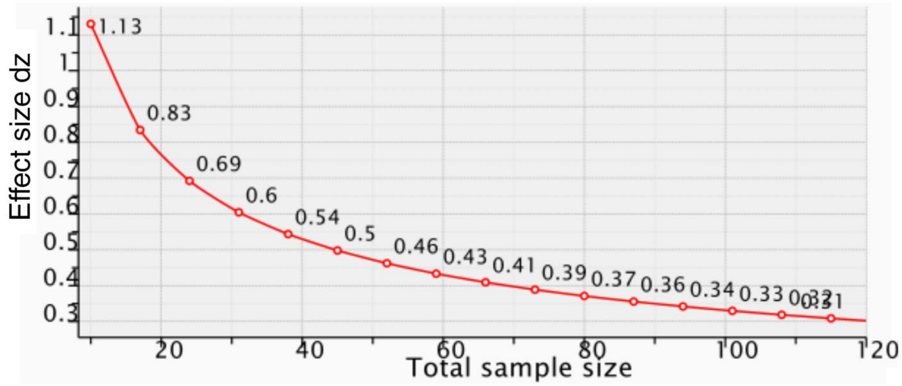

Figure 1. Power analysis chart to determine sample size.

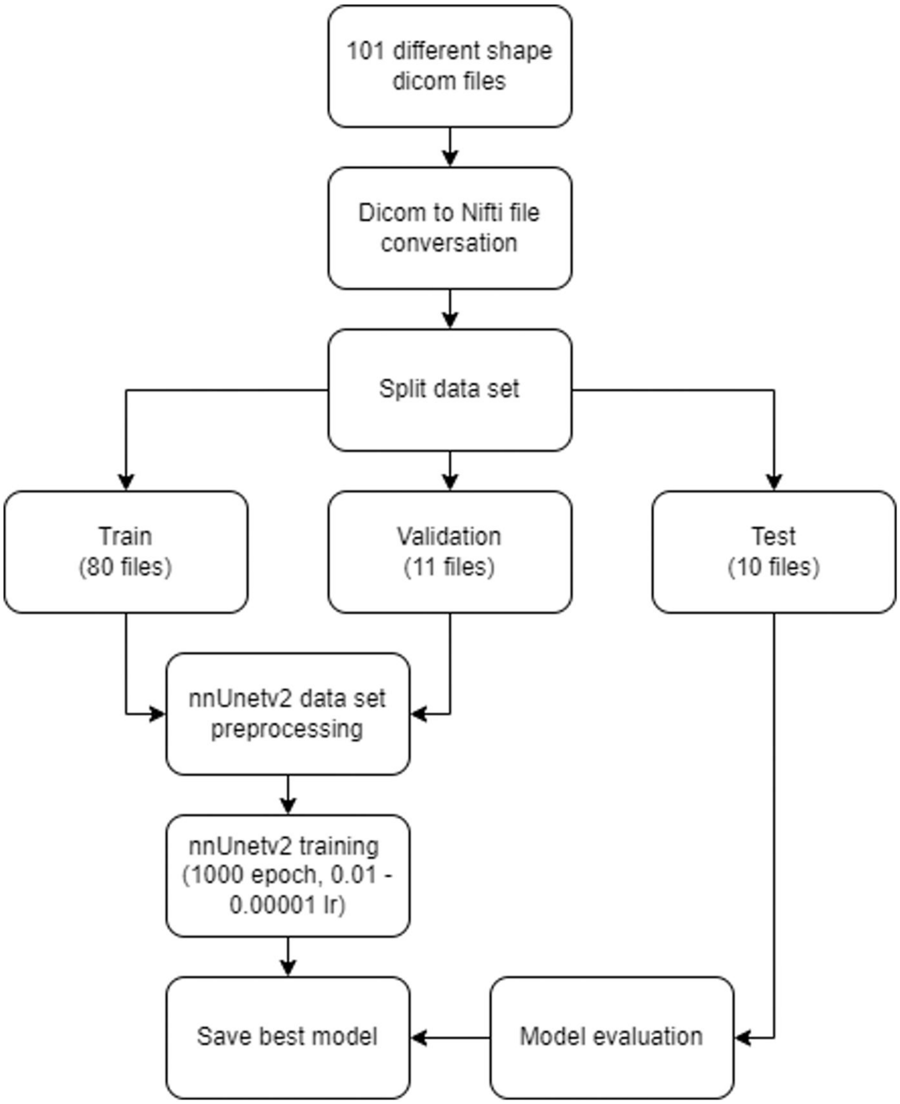

Figure 2. Model pipeline of automatic maxillary sinus segmentation.

high-resolution capabilities. CBCT is particularly useful for evaluating implant sites, especially in complex cases that require 3-dimensional images. In certain clinical scenarios, CBCT offers advantages over conventional PRs and CT scans.[4,10] After CT and magnetic resonance imaging transformed the way otolaryngology and head and neck radiology imaged the MS, the dental profession's adoption of CBCT has revolutionized the investigation of the maxillofacial region.[1]

Segmenting organs and tissues to create 3-dimensional models is a useful technique for diagnosis, surgical planning, and

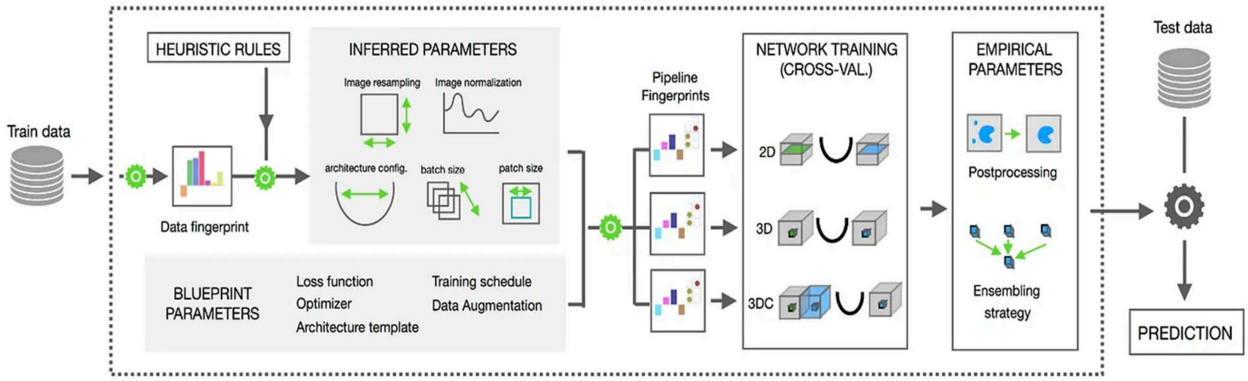

Figure 3. The nnU-Net v2 workflow.

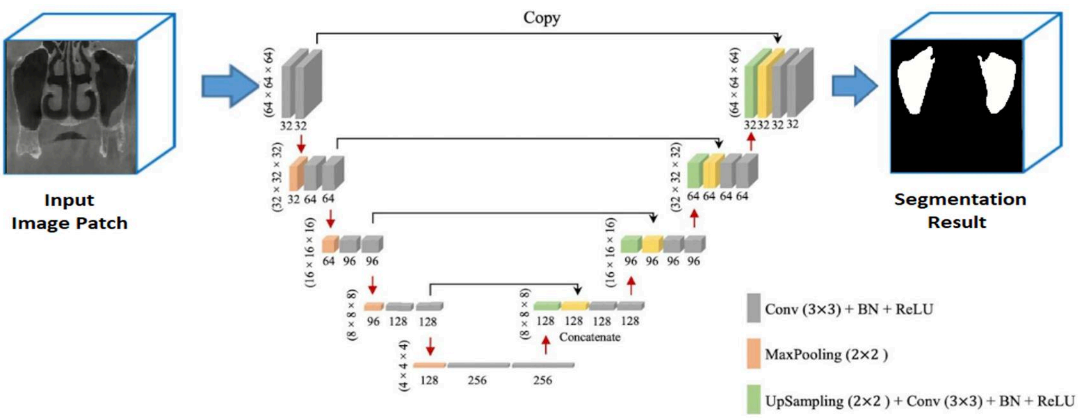

Figure 4. The nnU-Net v2 model algorithm.

simulation.[11] This technique is also applicable to the MS, which plays a significant part in oral and maxillofacial surgery. Segmentation of the MS enables accurate measurement of its volume, providing clinicians with quantitative insight into changes caused by cysts and tumours. In addition, accurately segmenting of the MS provides valuable guidance for clinicians when planning sinus lift elevation during implant surgery.[12] Although manual segmentation can be used for this purpose, it is time-consuming and dependent on the practitioner's experience due to high inter and intra-observer variability on CBCT images.[13] While semiautomated segmentation is generally more successful and easier to perform than manual segmentation, it still requires manual adjustments that may cause errors.[14] Moreover, segmentation of the MS on CBCT images is not an easy task due to CBCT-related reasons such as image noise, low soft tissue contrast, beam hardening artefacts and lack of absolute Hounsfield unit calibration. Furthermore, segmenting the MS can be a difficult task, particularly for nonspecialists, due to its close proximity to the nasal passages and tooth roots, anatomical variations, and frequent thickening of the sinus mucosa.[15] To overcome this issue, many studies have been reported to develop MS segmentation methods using computer-aided diagnosis systems and convolutional neural networks (CNNs) have emerged as preferred method for segmentation due to their high-quality results.[14,16] In 1 study, Jung et al[17] used Neural Networks U-Net (nnU-Net) to differentiate between air and lesions in the maxillary sinus on CBCT. In another study, Choi et al[12] developed a U-Net algorithm to automatically segment the maxillary sinus at varying levels of clarity and haze on CBCT. Morgan et al[15] also created a novel automatic U-Net method for maxillary sinus segmentation on CBCT.

One of the CNNs is nnU-Net v2, a deep learning-based segmentation method that is open source and automatically configures itself, including preprocessing, network architecture, training and postprocessing, to achieve competitive results without the need for expert knowledge.[18] To our knowledge, no previous study has evaluated automatic MS segmentation using nnU-Net v2. The objective of this study is to develop a CNN algorithm using nnU-Net v2 architecture and to evaluate its performance in automatically segmenting the MS on axial CBCT images.

Methods

Study design

In this retrospective study, a nnU-Net v2 based algorithm was developed using the Pytorch library at Python for the automatic segmentation of the MS in CBCT volumes. In this study, Checklist for Artificial Intelligence in Medical Imaging (CLAIM) and Standards for the Reporting of Diagnostic Accuracy Studies (STARD) Checklist were followed for preparing the manuscript. The noninterventional Clinical Research Ethical Committee of Eskişehir Osmangazi University approved the study protocol (decision no. 04.10.2022/22). The study was

Table 1. Metrics used to evaluate the performance of the nnU-Net v2 model, and the results obtained.

Metrics	Definition	Mathematic formula	Results
True positive (TP)	At least 50% of the voxels intersect between the automatic segmentation algorithm and the ground truth.		11377647
False positive (FP)	At least 50% of the voxels of the automatic segmentation algorithm do not intersect with the ground truth.		338009
False negative (FN)	At least 50% of the voxels of the ground truth do not intersect with the results of the automatic segmentation algorithm.		432827
Accuracy	Measures the overall correctness of predictions made by a model. It is the ratio of correctly predicted instances to the total number of instances in the dataset. A higher accuracy value signifies that the model has made a greater proportion of correct predictions among all instances in the dataset.	TP/(TP+FP+FN)	0.9993357789286772
Sensitivity (Recall)	Measures the algorithm's capacity to capture and correctly classify actual positive instances. Higher sensitivity values indicate a heightened ability of the algorithm to successfully detect positive instances within the dataset.	TP/(TP + FN)	0.9631128066389163
Precision	It measures the proportion of instances predicted as positive that are truly positive. A higher precision value indicates that the model is making fewer false positive predictions.	TP/(TP + FP)	0.9664285426968607
F1-score	This provides a balance between precision and recall. The F1 score is a measure of this balance, with a higher score indicating better overall performance of the model.	2TP/(2TP + FP + FN)	0.9619632388942536
Dice coefficient (DC)	Set A typically represents the pixels marked as part of the predicted segmentation by an algorithm, and Set B represents the pixels marked as the ground truth. The intersection is the number of overlapping pixels between the predicted and true segmentations. 0 indicates complete dissimilarity and 1 indicates complete similarity.	$2\|A \cap B\|/(\|A\|+\|B\|)$	0.9643270665242655
95% Hausdorff distance (95% HD) (mm)	Measures the distance between the furthest point in 1 set and the nearest point in the other set, and conversely. A lower value indicates a better spatial correspondence between the prediction segmentation and the ground truth.	$d_{H95}(A, B)=max(d_{95}(A, B), d_{95}(A, B))$	1.1903930636472058
Intersection over Union (IoU)	Measures the degree of overlap between the predicted and ground truth regions. 0 indicates no overlap between the predicted and ground truth regions, and 1 indicates perfect overlap.	$(\|A \cap B\|)/(\|A \cup B\|)$	0.9318588092908401

conducted in accordance with the principles of the Declaration of Helsinki.

Sample size calculation

Based on the power analysis conducted to determine the sample size, it was concluded that reliable results could be obtained with 101 cases using a paired 2-sample *t*-test, with 95% power and a 5% margin of error, and an effect size of dz = 0.31 (Figure 1).[19,20]

Patient selection

In the study, CBCT volumes obtained from individuals having healthy MS with no inflammatory findings were included from the radiology archive of the Department of Oral and Maxillofacial Radiology of Eskişehir Osmangazi University. The study excluded radiographic images that contained motion artefacts, metal artefacts, or those in which the affected area could not be accurately selected for MS segmentation. No differences were observed in age, gender, or ethnicity, and the data was anonymized before uploading into the labelling system.

Radiographic dataset

The scans were acquired using a Planmeca Promax 3D Mid CBCT device (Helsinki, Finland) with a field of view (FOV) of 23 × 17.3 cm and 0.400 mm voxel size. The acquisition parameters were 94 kVp, 14 mA, 360° rotation and 27 s exposure time. The patient data was converted to volumetric data and exported in DICOM file format, and can be viewed in sagittal, coronal, and axial slices. Although the spacing between the slices in the CBCT volumes was 0.2 mm, the volumes were exported at 1 mm intervals to avoid affecting the

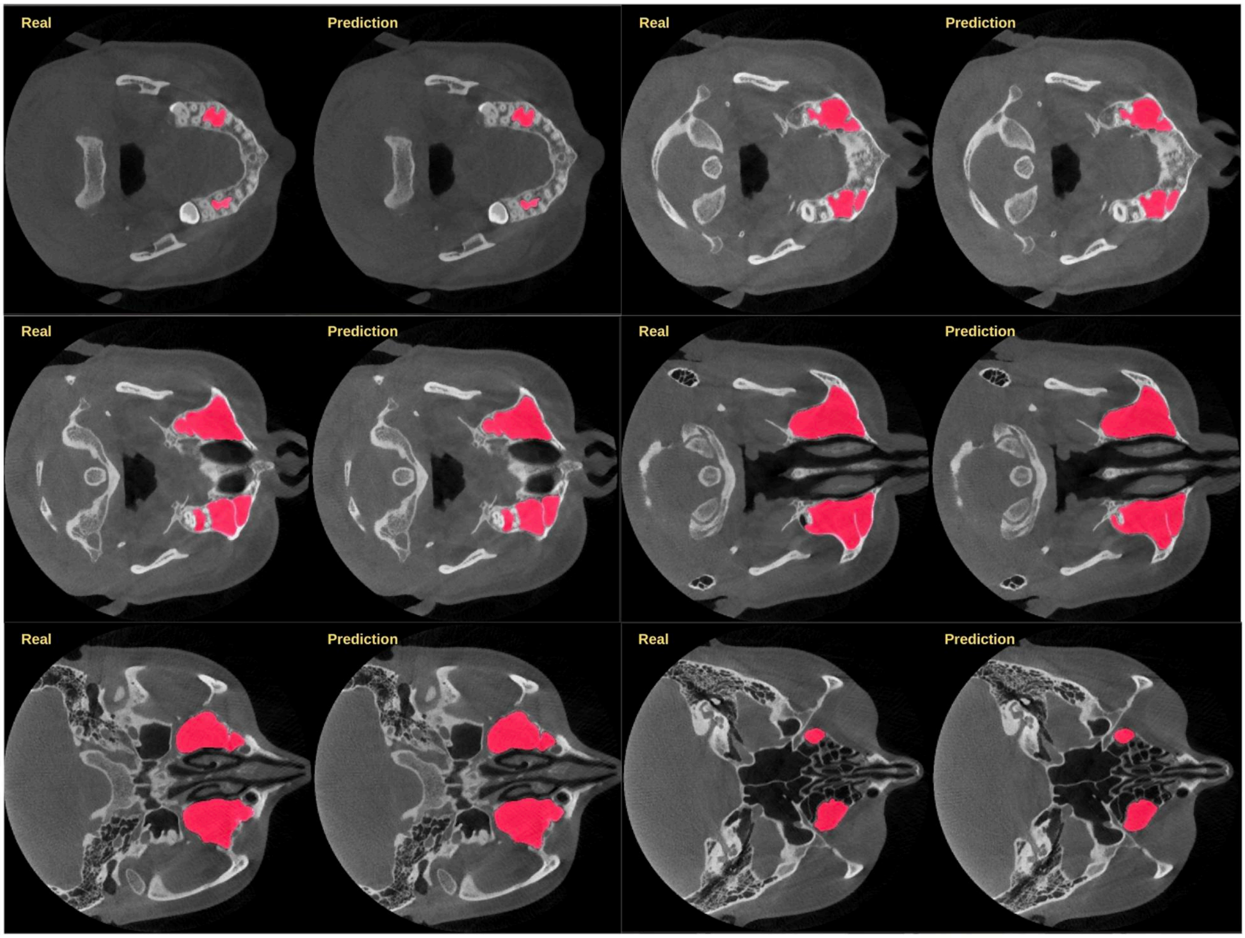

Figure 5. The automatic segmentation of the maxillary sinus utilizing the artificial intelligence model in axial CBCT slices.

model's performance, as neighbouring slices would be similar. The DICOM files were converted to the Neuroimaging Informatics Technology Initiative (NIfTI) format using a special code developed by the CranioCatch Software Team in Python programming language, with Pydicom, Nibabel, and Opencv libraries.

Ground truth

The CranioCatch Annotation Tool (CranioCatch, Eskisehir, Turkey) was used to label the MS on the axial CBCT volumes using a polygonal box segmentation technique. The ground truth was determined by the consensus of 2 experts in oral and maxillofacial radiology (N.S.E. and R.A.H.), both with at least 5 years of experience on CBCT. After the completion of all annotation process, labels were checked by seniors (at least 10 years' experience) oral and maxillofacial radiologist (I.S.B. and K.O.) with the exact agreement on all labels.

Data split

A total of 101 anonymized CBCT volumes with DICOM files were converted to NIfTI file format. The dataset was separated into the training (80%), validation (10%), and testing (10%) groups randomly.

1) Training group: 80 CBCT volumes
2) Validation group: 11 CBCT volumes
3) Test group: 10 CBCT volumes

Development of the nnU-Net v2 based CNN model

The automated MS segmentation algorithm, based on nnU-Net v2, was developed in the Python environment (v3.6.1; Python Software Foundation, Wilmington, DE, USA) using the PyTorch library. The model underwent training for 1000 epochs with learning rate of 0.00001 (Figure 2) Mathematical processing in the model's training was performed with a Dell PowerEdge T640 Calculation Server (Dell Inc., Round Rock, TX, USA), Dell PowerEdge T640 GPU Calculation Server (Dell Inc., Round Rock, TX, USA), and a Dell PowerEdge R540 Storage Server (Dell Inc., Round Rock, TX, USA) in the Eskişehir Osmangazi University Dentistry Faculty Dental-AI Laboratory, (Appendix).

The nnU-Net v2 workflow

The nnU-Net pipeline utilizes the heuristic rule to determine data-dependent hyperparameters, known as "data fingerprints," to retrieve training data. The pipeline fingerprints are formed by combining the plan parameters (loss function, optimizer, architecture) and inference parameters (image resampling, normalization, batch, and patch size) with the data fingerprint. These pipeline fingerprints generate network training for 2D, 3D, and 3D Cascaded U-Net using the hyperparameters determined thus far. The combination of various network configurations, along with postprocessing techniques, determines the optimal average "Dice coefficient" for the

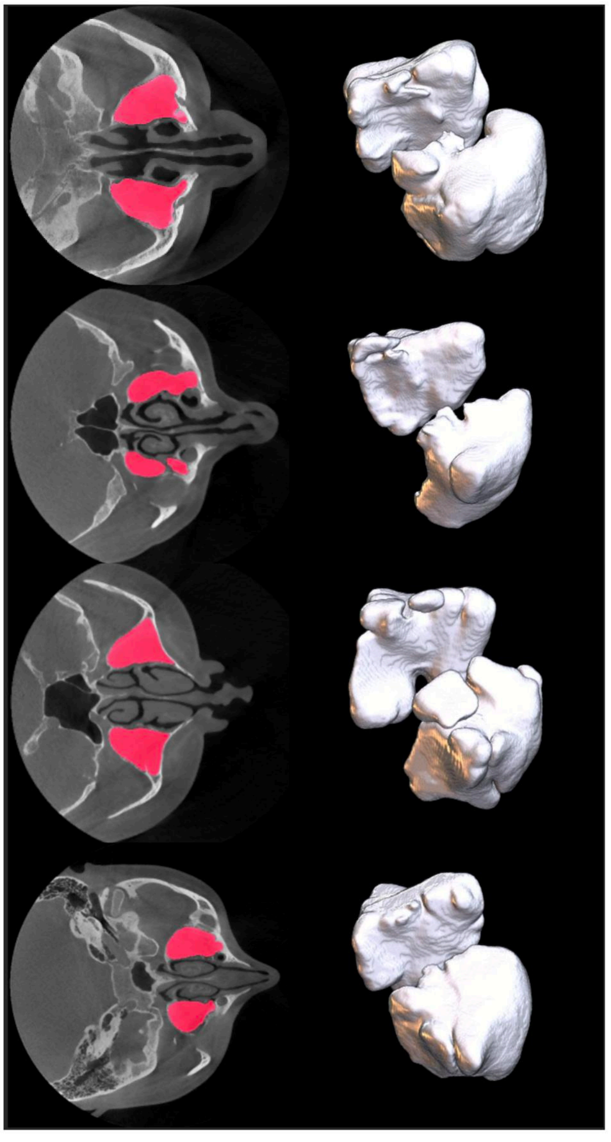

Figure 6. The nnU-Net v2 model was used to automatically segment the maxillary sinus, followed by a reconstruction process.

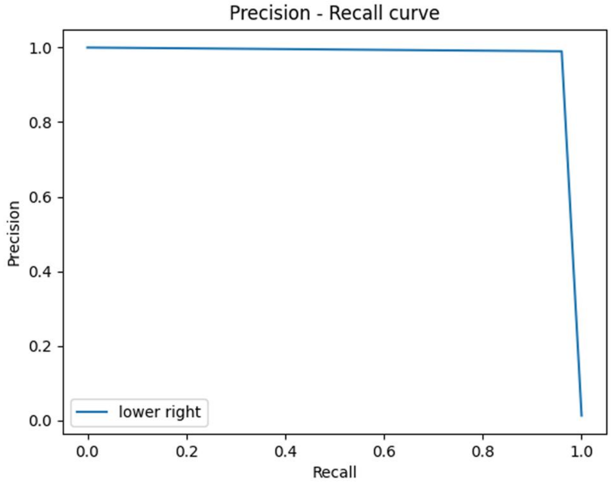

Figure 7. Precision-recall curve.

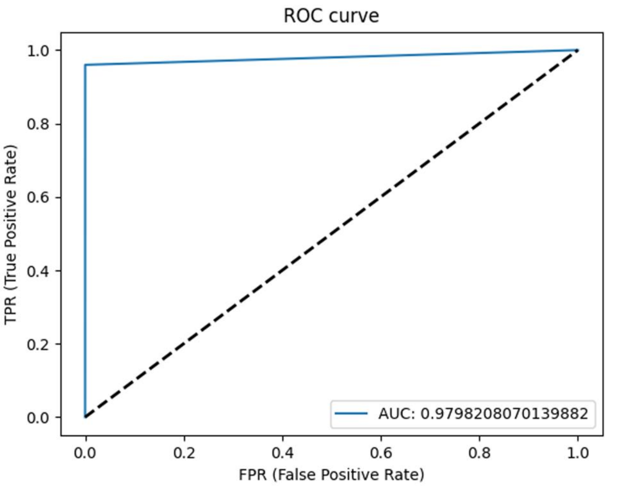

Figure 8. Receiver-operating characteristic (ROC) curve.

training data. The most effective configuration will then be utilized to produce predictions for the test data[18] (Figure 3).

The advantages of the nnU-Net v2 compared to older models

nnU-Net (Neural Networks U-Net) is an image segmentation model widely used in medical imaging applications. It is an enhanced version of the U-Net architecture that includes several important innovations, such as multiimage scaling, different data augmentation methods, and various loss functions. A key feature of nnU-Net is its configurability for a wide range of medical image segmentation problems. This allows for the creation of custom models tailored to specific data types, dimensions, and segmentation objectives. nnU-Net is a deep learning model that builds on the original U-Net architecture and incorporates several important innovations, including:

1) *Curly Paths:* nnU-Net introduces curly paths to the U-Net architecture, which are new connections that shorten the path between the output and input. This results in improved gradient flow during training and better outcomes.
2) *Dense Curly Paths:* nnU-Net densifies curly paths, allowing for deeper models and more feature maps, resulting in higher performance.
3) *Adaptive Skip Connections for Larger Scales:* nnU-Net introduces adaptive skip connections for larger scale images. This mechanism generates feature maps that cover a larger area for higher resolution images, resulting in improved outcomes.
4) *Loss Functions at Image and Voxel Level:* nnU-Net aims to achieve better results by using loss functions at both the image and voxel levels. This approach provides accurate results not only at the image level but also at the pixel or voxel level. nnU-Net achieves higher performance than the original U-Net due to these innovations.[18] This study evaluates the effectiveness of nnU-Net v2 in automatically segmenting MS (Figure 4).

Metrics for the model's performance

The model's performance in the automated segmentation of the MS on the axial CBCT scans was evaluated with F1-score, accuracy, sensitivity, precision, and area under curve (AUC)

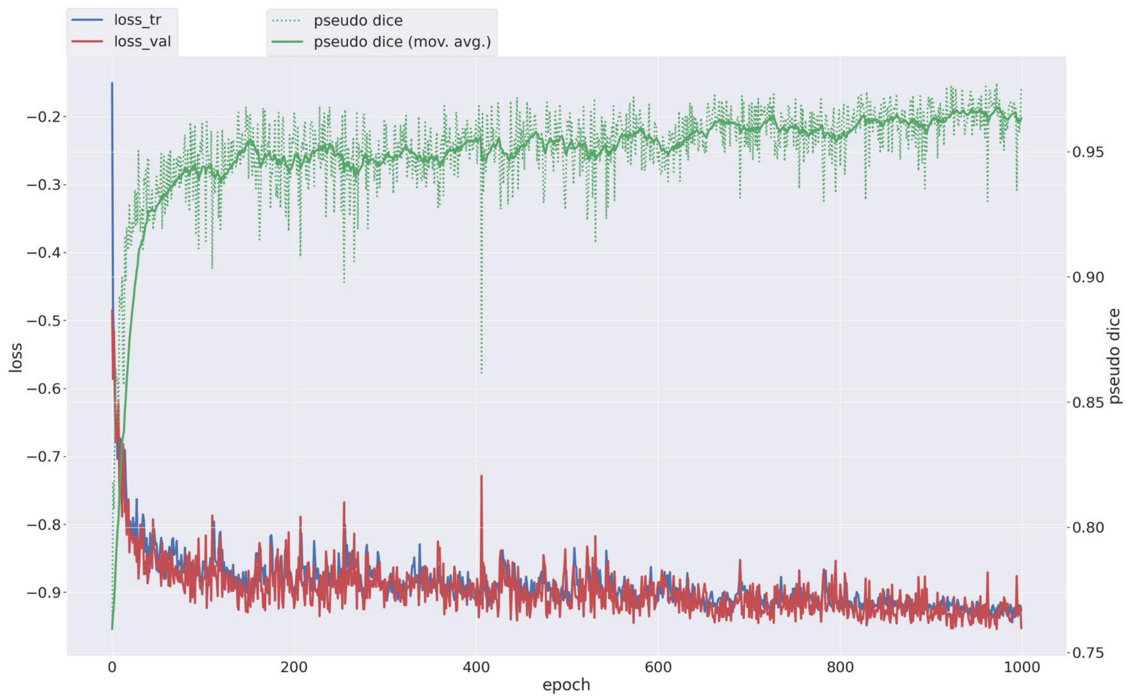

Figure 9. Evaluation of the overall loss functions and dice score was conducted during the 1000 rounds of training for the nnU-Net v2 dataset.

values. In addition, Dice coefficient (DC), 95% Hausdorff distance (95% HD), Intersection over Union (IoU) were measured (Table 1). The model's result was considered successful if the prediction and the ground truth intersected by more than 50% in each individual image slice. The true positive (TP), false positive (FP), and false negative (FP) results were determined for calculating the performance metrics. The definitions and the formulas for calculating the model's performance are described in Table 1.

Results

The algorithm based on nnU-Net v2 successfully predicted voxels belonging to the maxillary sinus with more than 50% intersection in almost all samples (Figures 5 and 6). The F1-score, accuracy, sensitivity, and precision values were found to be 0.96, 0.99, 0.96, and 0.96, respectively, indicating successful segmentation of the maxillary sinus in CBCT scans. DC, 95% HD, IoU values were 0.96, 1.19, 0.93, respectively. Table 1 presents the study results along with metric descriptions. The AUC value was found to be 0.97 (Figures 7-9).

Discussion

The use of AI in various fields, including medicine, is increasing due to innovations in deep learning technology. Deep learning algorithms have successfully addressed clinical problems in medicine, opening opportunities for their application in dentistry.[21] AI is employed across various dentistry domains to predict specific treatment outcomes and assist in diagnosis and treatment planning, particularly in dentomaxillofacial radiology. Its effectiveness in saving time and its ability to provide a valuable diagnostic assist to both experienced and less experienced dentists make it an important tool.[22]

CBCT is extensively utilized in dentistry for diagnosis, treatment planning, and surgery due to its capacity to offer comprehensive volumetric information about teeth and the surrounding alveolar bone, making it a valuable imaging modality compared to others.[23] CBCT has significantly improved the efficiency and accuracy of dental radiological diagnosis by producing higher quality images in less time and with lower radiation doses than CT. This has led to improved outcomes when treated appropriately.[24] However, despite these advantages, less experienced physicians have reported low inter-observer/intra-observer reliability when interpreting CBCT scans.[25] For this reason, automation is considered necessary for the segmentation of anatomical structures in CBCT images, which are frequently used in routine dentistry. The integration of AI into CBCT can facilitate and accelerate dental patient examinations, resulting in reduced physician workload and more reproducible and objective evaluations in a shorter time.[22]

AI is used in CBCT to detect various conditions such as periapical lesions,[26] second mesiobuccal canal,[27] and vertical root fractures in endodontics.[28] It is also used for implant planning based on the amount of alveolar bone[29] and inferior alveolar nerve canal detection[30] in implant surgery. In addition, it is used for the detection of intraosseous lesions,[31] temporomandibular disorders,[32] and automatic segmentation of the mandible[33] in oral and maxillofacial surgery. Furthermore, it assists cephalometric analysis in orthodontics.[34] Artificial intelligence is used for automatic tooth segmentation[35] and detection of mesiodens[36] in CBCT images.

The published literature on artificial intelligence studies of MS in CBCT images is limited, and information on these studies is summarized in Table 2. Jung et al[17] devised a 3-dimensional nnU-Net based algorithm aimed at segmenting the MS into lesion and air segments within CBCT images. The algorithm's development involved the implementation of an active learning model encompassing 3 iterative steps. Each successive model iteration not only refined its predecessor but also expanded the dataset, thereby augmenting performance in the face of

Table 2. Summary of the studies in the literature related to automatic segmentation of the maxillary sinus.

Study	Aim	Sample	Evaluation metrics	Segmentation method	Main findings
Bui et al[37]	The purpose of this study is to create a multistep scheme for automatic segmentation and reconstruction of the nasal cavity and paranasal sinuses from CBCT images using a coarse-to-fine active contour model.	10 patients	DC: 95.72% VOE: 8.73% Precision: 94.69% Recall: 97.73% F1-score: 95.72%	MATLAB and C++	This study demonstrates that the accuracy of the model developed for automatic segmentation of the nasal cavity and paranasal sinuses from the CBCT image of patients is higher than that of existing CBCT segmentation methods, such as Chan-Vese level set, localized Chan-Vese level set, and Bhattacharyya distance level set.
Neelapu et al[38]	The purpose of this study is to develop a new automatic segmentation algorithm for pharyngeal and sino-nasal airway subregions in 3D CBCT imaging datasets using knowledge-based algorithms and adaptive threshold segmentation.	15 patients	Precision: *min*: 86.66 ± 9.51—*max*: 99.44 ± 0.74 Recall: *min*: 83.44 ± 6.77—*max*: 97.75 ± 0.74 VOE: *min*: 3.92 ± 1.09—*max*: 14.93 ± 11.87 F1-score: *min*: 86.60 ± 8.95—*max*: 96.47 ± 3.44	MATLAB	This study tested 5 segmentation techniques, namely Chan-Vese Level Set, Localized Chan-Vese Level Set, Bhattacharya Distance Level Set, Grow Cut and Sparse Field Method for segmentation of airway subregions in both groups of patients with skeletal deformity and airway deformity. The overall F-score was greater than 80% for all airway sub-regions and the Sparse Field Method was found to give better results in all airways sub-regions compared to other methods.
Jung et al[17]	The purpose of this study was to evaluate the accuracy of the AI model by segmenting the maxillary sinus into air, and lesions, and to compare the results of the model with the segmentation performed by experts.	123 patients (103 patients-internal and 20 patients-external)	DC: 0.930 ± 0.16 (*Air*) DC: 0.760 ± 0.18 (*Lesion*)	nnU-Net	The study reported that the AI model achieved inferior results in lesion segmentation compared to air segmentation due to the varying radiopacities of maxillary sinus lesions. Additionally, the soft tissue wall thickness around the maxillary sinus varies from person to person, which can pose challenges in lesion segmentation. In conclusion, this study demonstrates that a deep learning algorithm based on nnU-net can efficiently reduce annotation efforts and costs by using a limited CBCT dataset.
Choi et al[12]	The purpose of this study is to develop a deep learning model for fully automated segmentation of the maxillary sinus in CBCT images with varying levels of clarity and haziness. Additionally, a postprocessing step will be added to the model to improve segmentation accuracy.	45 patients	DC: 0.9090 ± 0.1921 HD: 2.7013 ± 4.6154 Precision: 0.8977 ± 0.1874 Recall: 0.9282 ± 0.2005 *After postprocessing* DC: 0.9099 ± 0.1914 HD: 2.1470 ± 2.2790 Precision: 0.8999 ± 0.1860 Recall: 0.9282 ± 0.2005	U-Net	This research has demonstrated effective results in efficiently segmenting both clear and hazy maxillary sinuses using a deep learning algorithm that incorporates postprocessing techniques. The developed model exhibits promising capabilities and requires minimal time and effort. The developed artificial intelligence model promises to support dentists in accurately segmenting the maxillary sinuses in various cases when working with CBCT images.

(continued)

Table 2. (continued)

Study	Aim	Sample	Evaluation metrics	Segmentation method	Main findings
Morgan et al[15]	The purpose of this study was to create and test a novel automated CNN-based method for maxillary sinus segmentation on CBCT images.	132 patients	DC: 0.984 ± 0.004 IoU: 0.968 ± 0.008 %95 HD: 0.232 ± 0.059 RMS: 0.209 ± 0.072 *After postprocessing* DC: 0.996 ± 0.004 IoU: 0.992 ± 0.007 95% HD: 0.109 ± 0.115 RMS: 0.214 ± 0.123	U-Net	The study found that the U-net based CNN model successfully segmented the maxillary sinuses in CBCT images with high precision, reliability, and efficiency.
Çelebi et al[16]	The purpose of this study is to develop a pixel-based model for the diagnosis of maxillary sinus disorders since pixel-based methods are important in diagnosis and treatment by determining the boundaries of the diseased or healthy region investigated in health research.	315 patients	IoU: 81.42% F1-score: 89.76% Precision: 93.06% Recall: 86.68% Accuracy: 99.85% AUC: 98.79%	Swin-UNet-Res18	Experimental studies have shown that the ResNet 101 network gives the best results in sinus detection, and the Res-Swin-UNet model in this study outperforms the most recent studies. As a result, the proposed Res-Swin-UNet has achieved good results in defect detection problems such as background similarity and small defect size.
			IoU: 83.33% F1-score: 90.90% Precision: 89.76% Recall: 92.08% Accuracy: 99.86% AUC: 99.36%	Swin-UNet-Res34	
			IoU: 84.14% F1-score: 91.39% Precision: 91.20% Recall: 91.58% Accuracy: 99.87% AUC: 98.92%	Swin-UNet-Res50	
			IoU: 84.71% F1-score: 91.72% Precision: 91.57% Recall: 91.87% Accuracy: 99.87% AUC: 98.18%	Swin-UNet-Res101	
Present Study	The purpose of this study is to assess the performance of the model developed using the nnU-Net v2 architecture, an improved version of U-Net, in automatically segmenting the maxillary sinus on CBCT images.	101 patients	Accuracy: 0.99933 Recall: 0.96311 Precision: 0.96642 F1-score: 0.961963 DC: 0.96432 95% HD: 1.19039 IoU: 0.93185 AUC: 0.97982	nnU-Net v2	According to the data obtained as a result of this study, nnU-Net v2 has achieved high success in terms of automatic segmentation of the maxillary sinus in CBCT images. Automatic segmentation of the maxillary sinus, which has a critical importance in dentomaxillofacial surgery, is clinically important for dentists as well as other surgical branches related to this region.

Abbreviations: AUC = area under curve; DC = Dice coefficient; HD = Hausdorff distance; IoU = Intersection over Union; RMS = root mean square distance; VOE = volumetric overlap error constrained data availability. The reported DCs for the air and lesion segmentation stages were documented as 0.920 ± 0.17, 0.925 ± 0.16, and 0.930 ± 0.16, as well as 0.770 ± 0.18, 0.750 ± 0.19, and 0.760 ± 0.18, respectively. In their study, Çelebi et al[16] developed 4 deep learning algorithms, Swin-UNet-Res18, Swin-UNet-Res34, Swin-UNet-Res50, and Swin-UNet-Res101. The aim of the study was to identify pathological conditions related to MS in CBCT images using a new UNet structure based on ResNet and Swin Transformer. The study found that both Swin-UNetRes50 and Swin-UNet-Res101 models outperformed the other models with 99.87% accuracy. Swin-UNet-Res34 and Swin-UNet-Res18 followed with 99.86% and 99.85% accuracy, respectively. The most successful model, Swin-UNet-Res101, achieved an IoU of 84.71, F1-score of 91.72, precision of 91.57, recall accuracy of 91.87, and an AUC value of 99.18. In their study aimed at automatically segmenting the paranasal sinuses and nasal cavity on CBCT images, Bui et al[37] reported DC, precision, recall, and F1-score values of 95.72%, 94.69%, 97.73%, and 95.72%, respectively. Neelapu et al[38] proposed an algorithm for the fully automatic segmentation of pharyngeal and sino-nasal airway subregions in CBCT images. They compared 5 segmentation techniques and reported Dice Similarity Coefficient (DSC) and F1-score values ranging from 80 to 90% for all segmentation methods. Choi et al[12] developed a deep learning model using U-Net to segment 90 MS in CBCT images, including 34 clear and 56 hazy MS. The average DC and HD prediction results of U-Net were 0.9090 ± 0.1921 and 2.7013 ± 4.6154, respectively. Postprocessing was applied to eliminate prediction errors, resulting in improved DC and HD values of 0.9099 ± 0.1914 and 2.1470 ± 2.2790, respectively. Morgan et al[15] developed an automatic 3-dimensional U-Net algorithm for MS segmentation in CBCT images. The model accurately identified the segmented region with a DC of 98.4%.

When compared to similar studies in the literature, it was observed that 2 studies developed a U-Net based model and obtained high performance results similar to those obtained in this study.[12,15] Additionally, a study using nnU-Net found that the model developed by Jung et al[17] had difficulty detecting sinus lesions but was able to detect air in the sinus at a high rate. Çelebi et al[16] developed 4 different models using ResNet and Swin Transformer-based U-Net algorithms. The most successful model achieved automatic MS segmentation with high accuracy, similar to other studies in the literature and our own study. Our study is the first to perform automatic segmentation of the MS in CBCT volumes using nnU-Net v2, an upgraded version of U-Net, and it has achieved high accuracy values of 0.99. The results demonstrate that nnU-Net v2 is a dependable tool for automatic segmentation of the MS in CBCT images. However, the study is limited using images from a single tomography device and the focus on MS segmentation only. Future research should aim to develop deep learning algorithms that incorporate MS pathologies into the segmentation process. Additionally, these evaluations should be conducted using CBCT images acquired from a range of tomography devices with varying parameters.

In conclusion, the nnU-Net v2 based CNN developed in this study achieved high performance in automatically segmenting the maxillary sinus in CBCT images. Our results suggest that automatic segmentation of the maxillary sinus in CBCT images has the potential to significantly contribute to clinical decision-making, increase dentists' attention during examinations, and facilitate diagnosis and treatment processes while optimizing time efficiency.

Funding

The author(s) declare no financial support was received for the research, authorship, and/or publication of this article.

Conflicts of interest

None declared.

Appendix

The Eskisehir Osmangazi University Faculty of Dentistry's Dental Artificial Intelligence (AI) Laboratory has advanced technology computer equipment including a Dell PowerEdge T640 Calculation Server (Intel Xeon Gold 5218 2.3G, 16C/32T, 10.4 GT/s, 22M Cache, Turbo, HT [125 W] DDR4-2666, 32 GB RDIMM, 3200 MT/s, Dual Rank, PERC H330+ RAID Controller, 480 GB SSD SATA Read Intensive 6 Gbps 512 2.5in Hot-plug AG Drive); PowerEdge T640 GPU Calculation Server (Intel Xeon Gold 5218 2.3G, 16C/32T, 10.4 GT/s, 22M Cache, Turbo, HT [125 W] DDR4-2666 2, 32 GB RDIMM, 3200 MT/s, Dual Rank, PERC H330+ RAID Controller, 480 GB SSD SATA Read Intensive 6 Gbps 512 2.5in Hot-plug AG Drive, NVIDIA Tesla V100 16G Passive GPU); PowerEdge R540 Storage Server (Intel Xeon Silver 4208 2.1G, 8C/16T, 9.6 GT/s, 11M Cache, Turbo, HT [85 W] DDR4-2400, 16 GB RDIMM, 3200 MT/s, Dual Rank, PERC H730P+ RAID Controller, 2 Gb NV Cache, Adapter, Low Profile, 8 TB 7.2K RPM SATA 6Gbps 512e 3.5in Hot-plug Hard Drive, 240 GB SSD SATA Mixed Use 6 Gbps 512e 2.5in Hot plug, 3.5in HYB CARR S4610 Drive); Precision 3640 Tower CTO BASE Workstation (Intel (R) Xeon(R) W-1250P [6 Core, 12M cache, base 4.1 GHz, up to 4.8 GHz] DDR4-2666, 64 GB DDR4 [4 X16 GB] 2666 MHz UDIMM ECC Memory, 256 GB SSD SATA, Nvidia Quadro P620, 2 GB); Dell EMC Network Switch (N1148T-ON, L2, 48 ports RJ45 1GbE, 4 ports SFP+ 10GbE, Stacking).

References

1. Whyte A, Boeddinghaus R. The maxillary sinus: physiology, development and imaging anatomy. *Dentomaxillofac Radiol*. 2019;48(8):20190205.
2. Kim MJ, Jung UW, Kim CS, et al. Maxillary sinus septa: prevalence, height, location, and morphology. A reformatted computed tomography scan analysis. *J Periodontol*. 2006;77(5):903-908.
3. Yeung AWK, Hung KF, Li DTS, Leung YY. The use of CBCT in evaluating the health and pathology of the maxillary sinus. *Diagnostics (Basel)*. 2022;12(11):2819.
4. Shahbazian M, Vandewoude C, Wyatt J, Jacobs R. Comparative assessment of panoramic radiography and CBCT imaging for radiodiagnostics in the posterior maxilla. *Clin Oral Investig*. 2014;18(1):293-300.
5. Lopes LJ, Gamba TO, Bertinato JVJ, Freitas DQ. Comparison of panoramic radiography and CBCT to identify maxillary posterior roots invading the maxillary sinus. *Dentomaxillofac Radiol*. 2016;45(6):20160043.
6. Constantine S, Clark B, Kiermeier A, Anderson PP. Panoramic radiography is of limited value in the evaluation of maxillary sinus

disease. *Oral Surg Oral Med Oral Pathol Oral Radiol*. 2019;127(3):237-246.
7. Lang AC, Schulze RK. Detection accuracy of maxillary sinus floor septa in panoramic radiographs using CBCT as gold standard: a multi-observer receiver operating characteristic (ROC) study. *Clin Oral Investig*. 2019;23(1):99-105.
8. Vollmer A, Saravi B, Vollmer M, et al. Artificial ıntelligence-based prediction of oroantral communication after tooth extraction utilizing preoperative panoramic radiography. *Diagn Basel Switz*. 2022;12(6):1406.
9. Sekerci AE, Sisman Y, Etoz M, Bulut DG. Aberrant anatomical variation of maxillary sinus mimicking periapical cyst: a report of two cases and role of CBCT in diagnosis. *Case Rep Dent*. 2013;2013:757645.
10. Rege ICC, Sousa TO, Leles CR, Mendonça EF. Occurrence of maxillary sinus abnormalities detected by cone beam CT in asymptomatic patients. *BMC Oral Health*. 2012;12:30.
11. Andersen TN, Darvann TA, Murakami S, et al. Accuracy and precision of manual segmentation of the maxillary sinus in MR images—a method study. *Br J Radiol*. 2018;91(1085):20170663. Mar 20;
12. Choi H, Jeon KJ, Kim YH, Ha EG, Lee C, Han SS. Deep learning-based fully automatic segmentation of the maxillary sinus on cone-beam computed tomographic images. *Sci Rep*. 2022;12(1):14009.
13. Tingelhoff K, Eichhorn KWG, Wagner I, et al. Analysis of manual segmentation in paranasal CT images. *Eur Arch Otorhinolaryngol*. 2008;265(9):1061-1070. Sep
14. Xu J, Wang S, Zhou Z, Liu J, Jiang X, Chen X. Automatic CT image segmentation of maxillary sinus based on VGG network and improved V-Net. *Int J Comput Assist Radiol Surg*. 2020;15(9):1457-1465.
15. Morgan N, Van Gerven A, Smolders A, de Faria Vasconcelos K, Willems H, Jacobs R. Convolutional neural network for automatic maxillary sinus segmentation on cone-beam computed tomographic images. *Sci Rep*. 2022;12(1):7523.
16. Çelebi A, Imak A, Üzen H, et al. Maxillary sinus detection on cone beam computed tomography images using ResNet and Swin Transformer-based UNet. *Oral Surg Oral Med Oral Pathol Oral Radiol*. 2023;S2212-4403(23)00503-5.
17. Jung SK, Lim HK, Lee S, Cho Y, Song IS. Deep active learning for automatic segmentation of maxillary sinus lesions using a convolutional neural network. *Diagnostics (Basel)*. 2021;11(4):688.
18. Isensee F, Jaeger PF, Kohl SAA, Petersen J, Maier-Hein KH. nnU-Net: a self-configuring method for deep learning-based biomedical image segmentation. *Nat Methods*. 2021;18(2):203-211.
19. Cohen J. *Statistical Power Analysis for the Behavioral Sciences*. 2nd ed. Routledge; 1988.
20. Gibson E, Hu Y, Huisman HJ, Barratt DC. Designing image segmentation studies: Statistical power, sample size and reference standard quality. *Med Image Anal*. 2017;42:44-59.
21. Önder M, Evli C, Türk E, et al. Deep-learning-based automatic segmentation of parotid gland on computed tomography images. *Diagnostics (Basel)*. 2023;13(4):581. Jan
22. Mureșanu S, Almășan O, Hedeșiu M, Dioșan L, Dinu C, Jacobs R. Artificial intelligence models for clinical usage in dentistry with a focus on dentomaxillofacial CBCT: a systematic review. *Oral Radiol*. 2023;39(1):18-40.
23. Hung K, Montalvao C, Tanaka R, Kawai T, Bornstein MM. The use and performance of artificial intelligence applications in dental and maxillofacial radiology: a systematic review. *Dentomaxillofac Radiol*. 2020; 49(1):20190107.
24. Scarfe WC, Angelopoulos C. editors. *Maxillofacial Cone Beam Computed Tomography: Principles, Techniques and Clinical Applications [Internet]*. Springer International Publishing; 2018.
25. Parker JM, Mol A, Rivera EM, Tawil PZ. Cone-beam computed tomography uses in clinical endodontics: observer variability in detecting periapical lesions. *J Endod*. 2017;43(2):184-187.
26. Orhan K, Bayrakdar IS, Ezhov M, Kravtsov A, Özyürek T. Evaluation of artificial intelligence for detecting periapical pathosis on cone-beam computed tomography scans. *Int Endod J*. 2020;53(5):680-689.
27. Duman ŞB, Çelik Özen D, Bayrakdar IŞ, et al. Second mesiobuccal canal segmentation with YOLOv5 architecture using cone beam computed tomography images. *Odontology*. 2023;112(2):552-561.
28. Johari M, Esmaeili F, Andalib A, Garjani S, Saberkari H. Detection of vertical root fractures in intact and endodontically treated premolar teeth by designing a probabilistic neural network: an ex vivo study. *Dentomaxillofac Radiol*. 2017;46(2):20160107.
29. Sorkhabi MM, Saadat Khajeh M. Classification of alveolar bone density using 3-D deep convolutional neural network in the cone-beam CT images: A 6-month clinical study. *Measurement*. 2019;148:106945.
30. Cipriano M, Allegretti S, Bolelli F, et al. Deep segmentation of the mandibular canal: a new 3D annotated dataset of CBCT volumes. *IEEE Access*. 2022;10:11500-11510.
31. Abdolali F, Zoroofi RA, Otake Y, Sato Y. Automated classification of maxillofacial cysts in cone beam CT images using contourlet transformation and spherical harmonics. *Comput Methods Programs Biomed*. 2017;139:197-207.
32. Eşer G, Duman ŞB, Bayrakdar İŞ, Çelik Ö. Classification of temporomandibular joint osteoarthritis on cone beam computed tomography images using artificial intelligence system. *J Oral Rehabil*. 2023;50(9):758-766.
33. Qiu B, van der Wel H, Kraeima J, et al. Automatic segmentation of mandible from conventional methods to deep learning—a review. *J Pers Med*. 2021;11(7):629.
34. Torosdagli N, Liberton DK, Verma P, Sincan M, Lee JS, Bagci U. Deep geodesic learning for segmentation and anatomical landmarking. *IEEE Trans Med Imaging*. 2019;38(4):919-931.
35. Chen Y, Du H, Yun Z, et al. Automatic segmentation of individual tooth in dental CBCT images from tooth surface map by a multi-task FCN. *IEEE Access*. 2020;8:97296-97309.
36. Syed AZ, Çelik Ozen D, Abdelkarim AZ, et al. Automated mesiodens detection with deep-learning-based system using cone-beam computed tomography images. *Int J Intell Syst*. 2023;2023:e4415970-8.
37. Bui NL, Ong SH, Foong KWC. Automatic segmentation of the nasal cavity and paranasal sinuses from cone-beam CT images. *Int J Comput Assist Radiol Surg*. 2015;10(8):1269-1277.
38. Neelapu BC, Kharbanda OP, Sardana V, et al. A pilot study for segmentation of pharyngeal and sino-nasal airway subregions by automatic contour initialization. *Int J Comput Assist Radiol Surg*. 2017;12(11):1877-1893.

Dentomaxillofacial Radiology, 2024, 53, 256–266
https://doi.org/10.1093/dmfr/twae012
Research Article